Electronic Supplementary Material (ESI) for Lab on a Chip.

A versatile, cost-effective, and flexible wearable biosensor for *in situ* and *ex situ* sweat analysis, and personalized nutrition assessment

Zhong Zhang, Morteza Azizi, Michelle Lee, Peter Lawrence, Philip Davidowsky, Alireza Abbaspourrad*

Supporting Information

Department of Food Science, College of Agriculture and Life Sciences, Cornell University, Ithaca 14853, NY, USA

Correspondence: Alireza Abbaspourrad*, Department of Food Science, College of Agriculture and Life Sciences, Cornell University, Ithaca 14853, NY, USA. Tel: (607) 255-2923. Email: alireza@cornell.edu

This document contains 11 supplemental figures (**Fig. S1-S11**) and 1 supplemental table (**Table S1**).

Fig. S1 Microfluidic patterns designed for sweat collection and monitoring. (These designs were studied and screened for the best flow/sensing results. Number 9 were selected as the final design.)

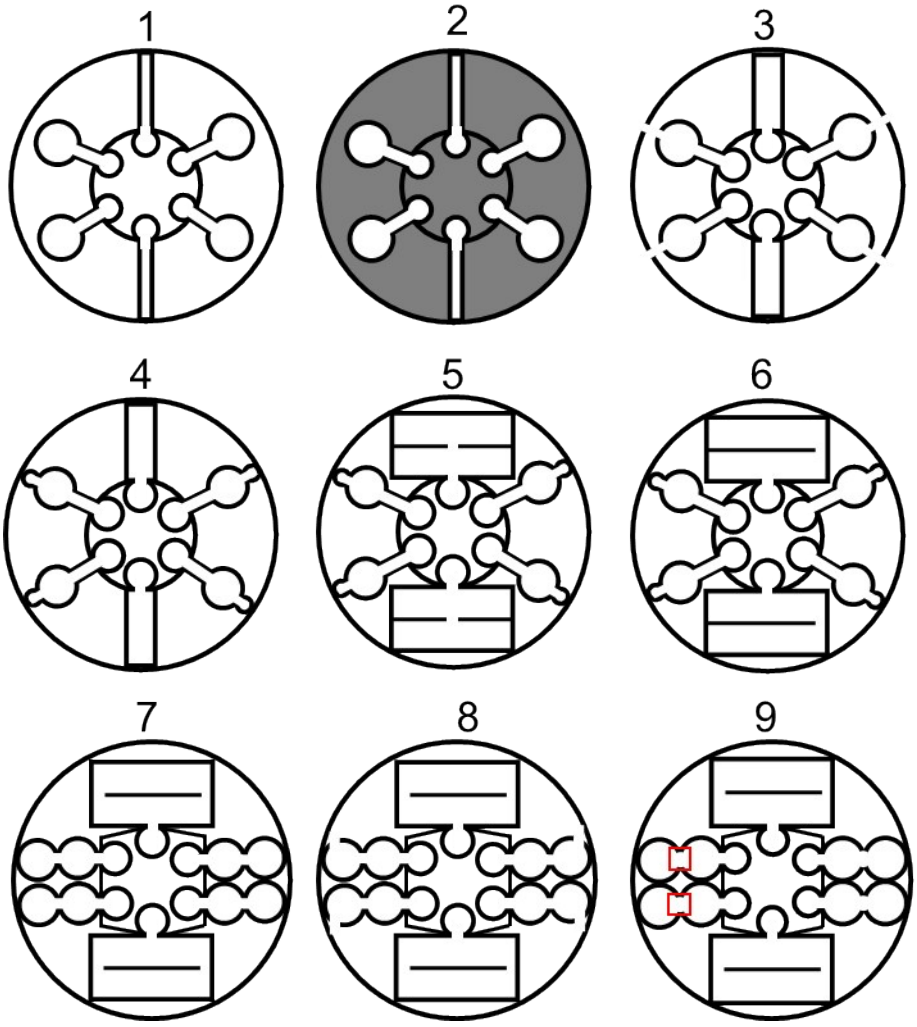

Due to the accessibility of human sweat, we have concepted the idea to collect the sweat non-invasively through a filter paper and measure the biomarkers of interests on the same device. The initial two patterns (#1 & #2) were developed to collect the human sweat through the six inlets located inside the inner circle. The capillary force of cellulose fibers and the perspiration pressure push the sweat to two sweat storage/monitoring zones, two glucose sensing zones, and two pH measuring zones. Two zones with exact same function were designed to minimize the variations and increase the accuracy. However, the sweat storage zone of design #1 and #2 was filled quickly with sweat (~1.5 μL) due to its small area and fast drawing of the capillary force. Design #2 was created to print more ink (wax) on the device to avoid the leaking of the sweat through boundaries. However, it was found that the melted wax boundaries on design #1 could hold the sweat without leaking.

We enlarged the sweat storage zone and created a venting channel on the patch which allows the sweat to escape from the detection zone and flow toward the boundary of the device in design #3. However, the defect of this design is that the sweat from outside could be introduced into the detection zone through vent. In design #4, we sealed the vent from design #3 and extended a small circle area on the sensing zones. It is hoped that the small circle area could help concentrate the color that is generated from the sensing reactions. But we could not achieve

the sensitivity to detect the glucose in the physiological concentrations (50 - 300 μM). We have further increased the sweat storage/sensing zone in design #5 and #6 in order to bring more sweat to the device and to the sensing zones. However, we have noticed a leaking of sweat in the glucose/pH sensing zones due to the excessive amount of sweat introduced. The difference between #5 and #6 is that the sweat flow into different directions after midline of the storage zone. We changed the design of sweat storage/volume sensing zone to design #7, #8, #9, which allows the sweat to flow more efficiently toward the storage zones, while providing a marker line in the middle to indicate when to stop the exercise. Meanwhile, the size of glucose/pH sensing zones were also increased to accommodate the higher sweat volume. Design #7 and #8 were eliminated because we found that the vent has to be created in the cover medical tape to let sufficient oxygen flow in, allow the sweat vapor to escape, and concentrate the colors in the red rectangle region in design #9.

Fig. S2 Process to print the microfluidic patterns on filter paper.

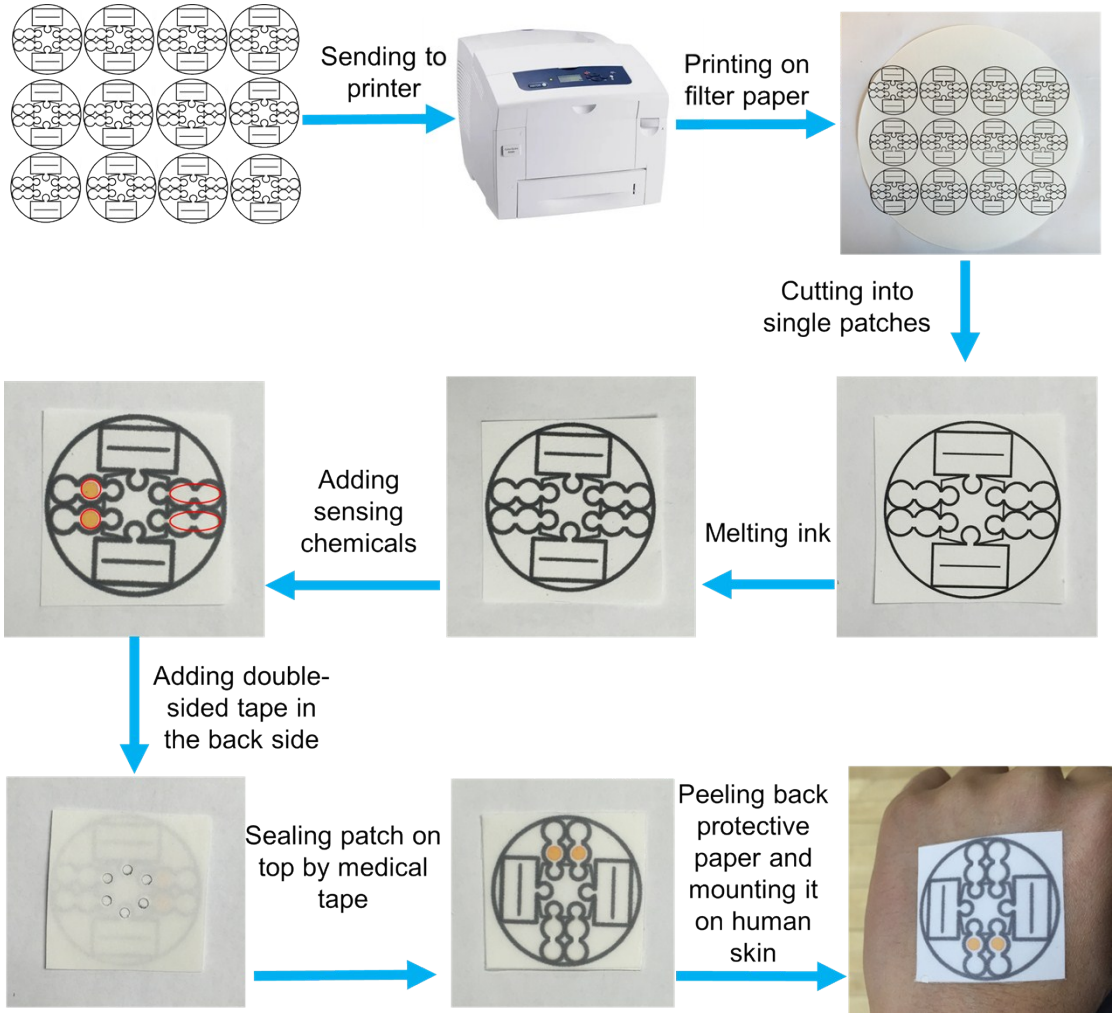

Fig. S3 Optical images of the patches of sweat apparent on the device, attached to a human hand, in different lighting exposures.

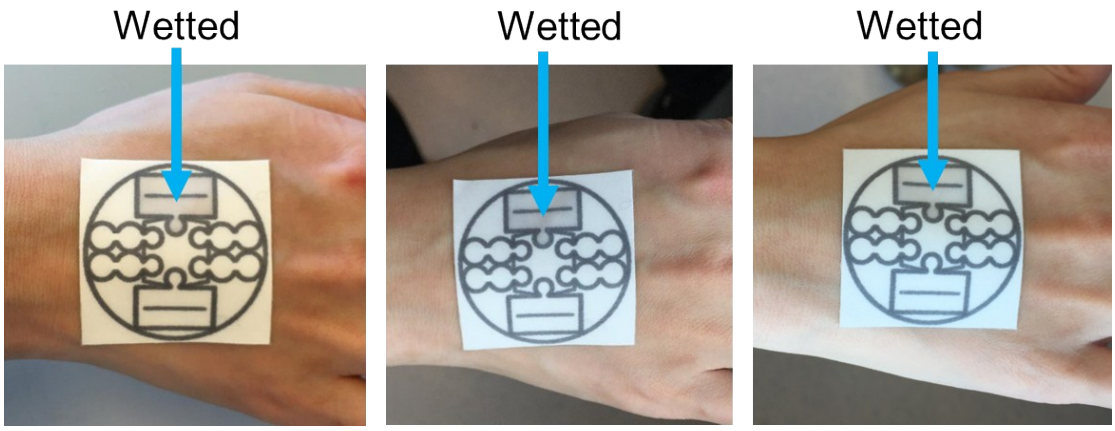

Fig. S4 Scanning electron microscopy image of the cellulose fibers that make up the filter paper. The approximate diameter of the cellulose fibers is ~15–20 μm.

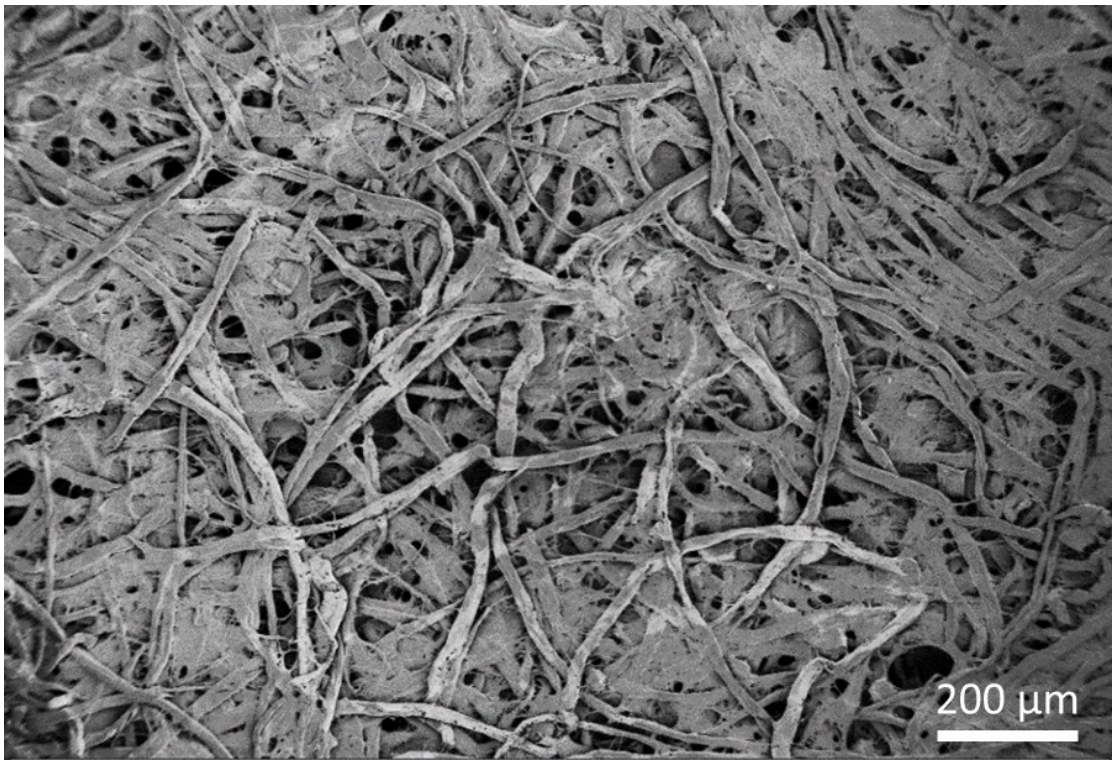

Fig. S5 Calculation of the wetted area for the sweat collection zones by ImageJ software. (The wetted area has to be hand-picked in the ImageJ software.)

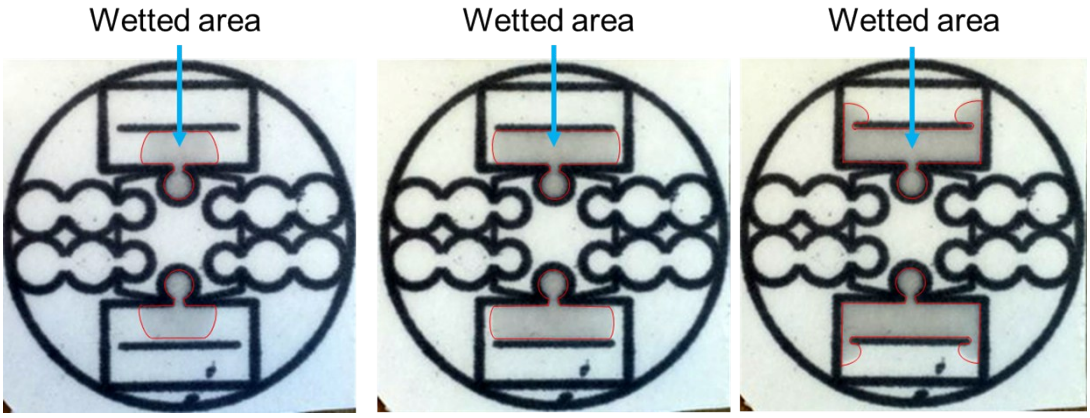

Fig. S6 Design of the glucose detection zone and the flow of sweat vapor and oxygen.

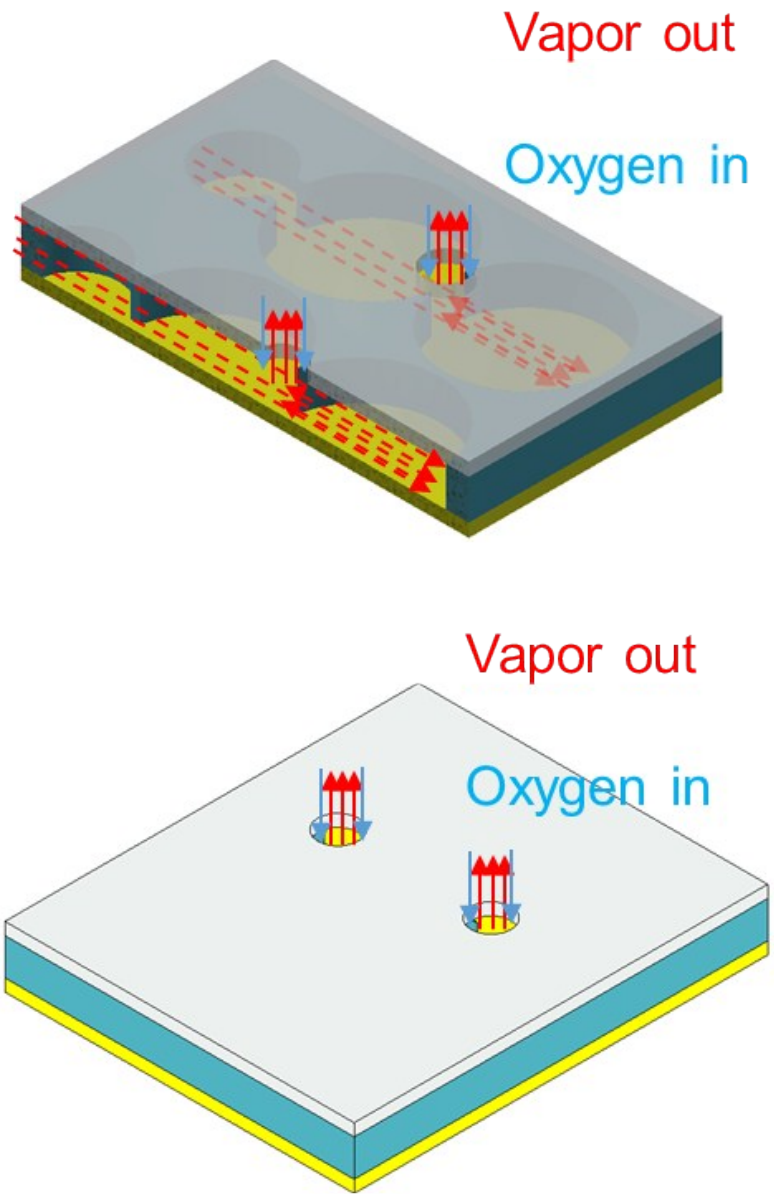

Fig. S7 Optical images of glucose detection zones without the venting design.

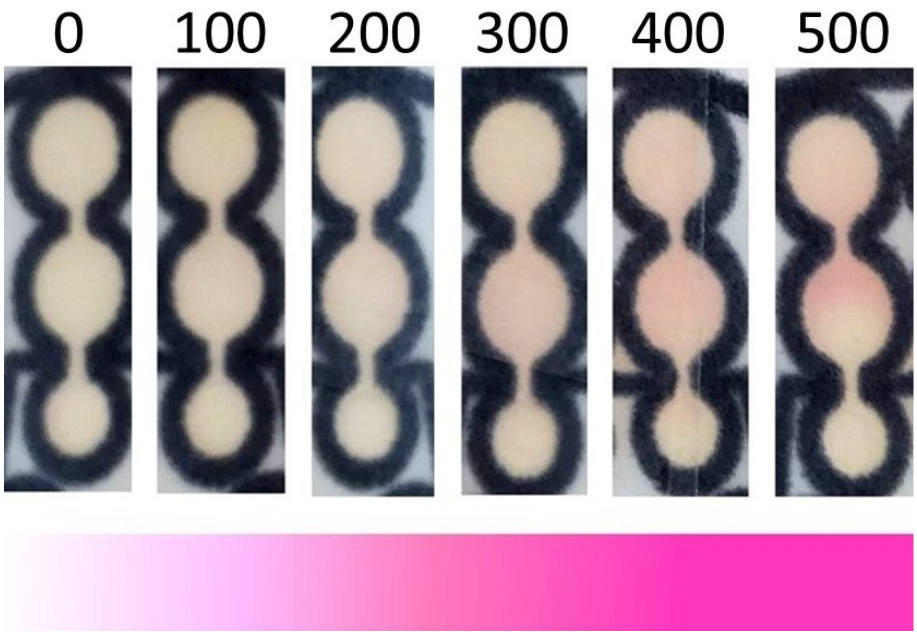

Fig. S8 Detection of lactate by other designs and sensing chemicals: (**A**), by a commercial lactate sensing kit with vent in the middle of the sensing zone (pink color did not concentrate in the venting zone; unknown color substrate used for the sensing reaction); **(B)**, by lactate oxidase/Peroxidase/AAP-DHBS with a vent on the top of the sensing zone (pink color concentrated in the venting zone.).

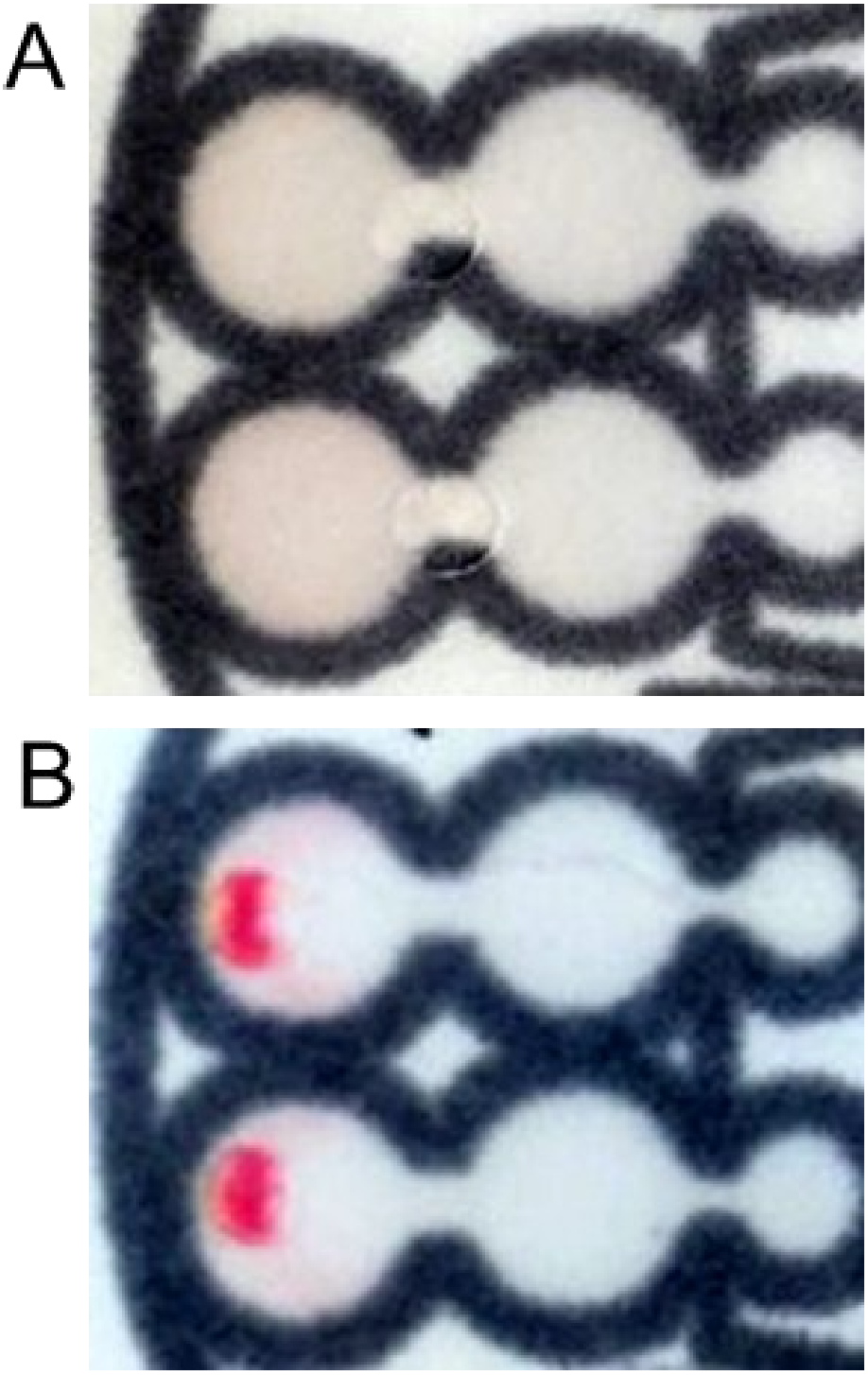

Fig. S9. Quantification of glucose in sweat when the photos of the device were taken from 3 inch, 4 inch, and 5 inch distances: (a), glucose standard curve determined by the color intensity of the glucose sensing zone; (b) glucose standard curve determined by the intensity ratio of the glucose sensing zone and the center of the wearable patch (control); (c), glucose standard curve determined by the intensity difference of the glucose sensing zone and the center of the wearable patch (control); (d), illustration of the designated control zone and the calculation equation.

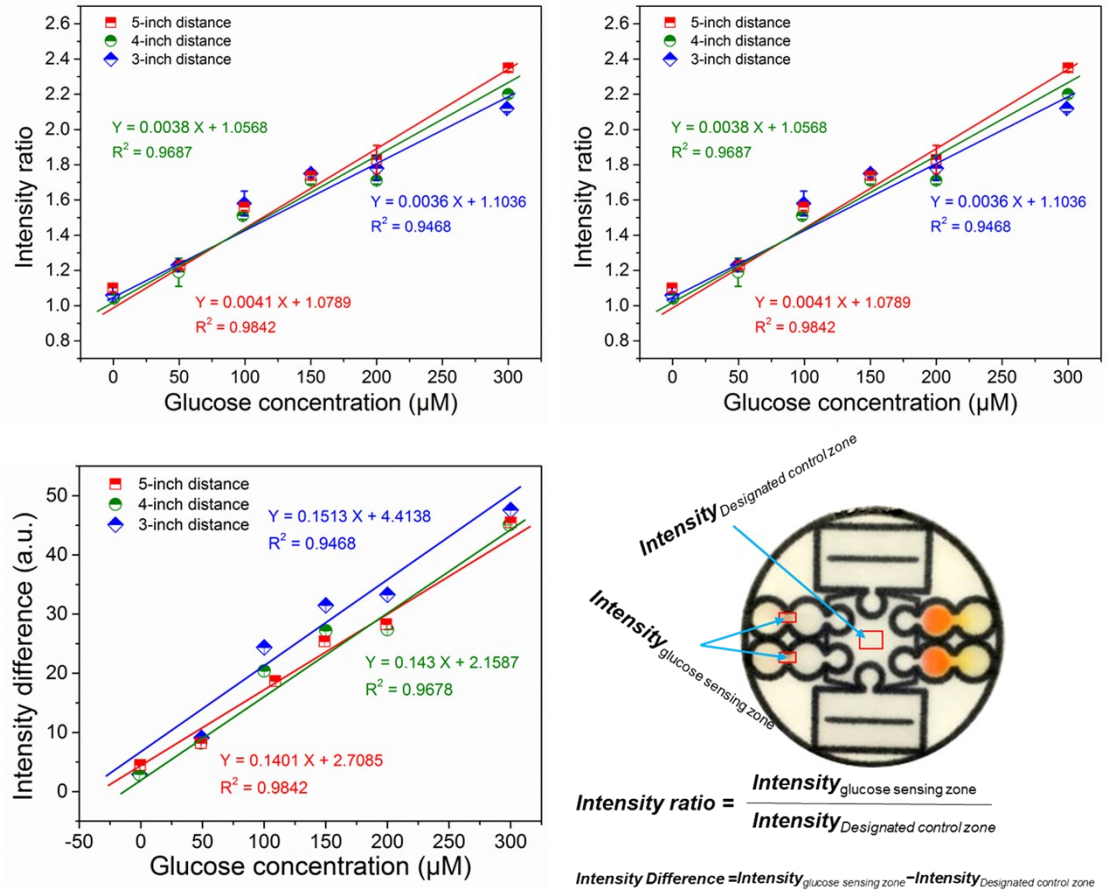

Fig. S10. Quantification of glucose in sweat when the photos were taken from weak, medium and strong lighting exposures: (a), glucose standard curve determined by the color intensity of the glucose sensing zone; (b) glucose standard curve determined by the intensity ratio of the glucose sensing zone and the center of the wearable patch (control); (c), glucose standard curve determined by the intensity difference of the glucose sensing zone and the center of the wearable patch (control); (d), illustration of the designated control zone and the calculation equation.

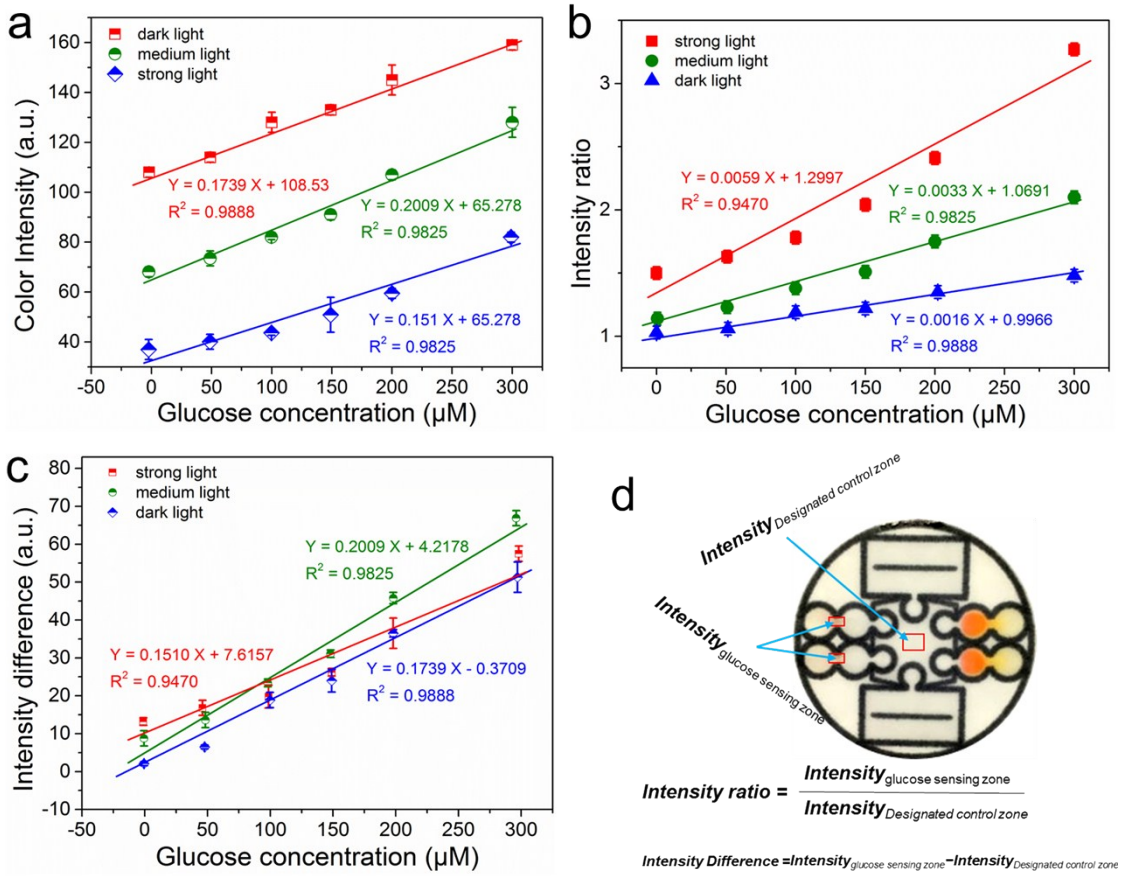

Fig. S11. Wearable device designed with two pH sensing zones, two sweat collection and sweat volume sensing zones, and two glucose sensing zones for human studies.

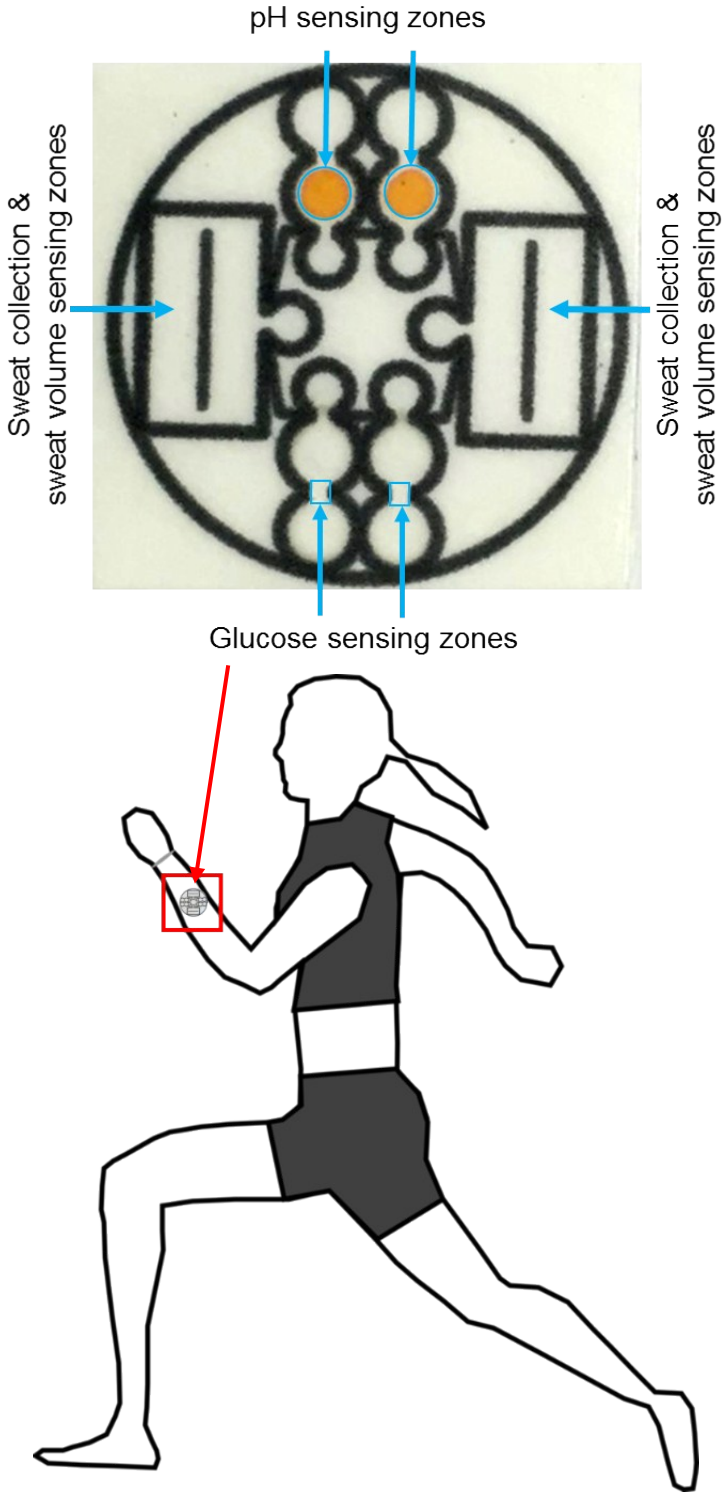

Table S1. Recovery study of the glucose spiked in simulate sweat

Added Concentration (μM)	Intensity of glucose zone (a.u.)	Intensity of control zone (a.u.)	Intensity Ratio (glucoe/control)	Predicted concentration of glucose (μM)	Average of Recovered glucose concenration (μM)	Standard Deviation (μM)	Recovery
0.0	41.13	39.46	1.04	-9.88	-13.79	5.52	-
0.0	39.96	39.46	1.01	-17.69			
50.0	54.30	42.02	1.29	55.88	67.08	15.84	134.2%
50.0	57.87	42.02	1.38	78.28			
200.0	61.33	36.85	1.66	153.81	200.29	46.48	100.1%
200.0	74.35	36.85	2.02	246.77			
300.0	76.67	35.03	2.19	291.88	322.35	43.09	107.4%
300.0	84.78	35.03	2.42	352.81			

Calculation Method:

If the sweat volume is different than 7.5 μL (a volume used to build the standard curve): the sweat collection zone shows X μL of sweat, then the concentration of glucose is corrected by a factor of 7.5/X since the standard curve is built based on 7.5 μL of sweat.

Example 1, if 5.0 μL of sweat shows in the sweat collection zone and the calculated concentration of glucose based on the intensity ratio and standard curve is 100.00 μM, the true concentration of glucose is corrected to:

$$\text{Corrected concentration of glucose} = 100.00 \times 7.5/5.0 = 150.00\ \mu M$$

Example 2, if 10.0 μL of sweat shows in the sweat collection zone and the calculated concentration of glucose based on the intensity ratio and standard curve is 100.00 μM, the true concentration of glucose is corrected to:

$$\text{Corrected concentration of glucose} = 100.00 \times 7.5/10.0 = 75.00\ \mu M$$

Table S2. LC-MS analysis of the sweat extracted from the patch in human studies. The nutrients were determined by their individual molecule weight and mass profiles.

Target Molecule	LS-MS area
Lactate	3386.0
Creatine	751747.5
Choline Chloride	27153.5
Aspartic acid	71862.5
Glutamic acid	474938.0
Arginine	396983.5
Ascorbic acid	702772.5
Glucose	19102.5
Thiamine	30047.5
Riboflavin	152614.0
Folic acid	115559.5